



## Original Research Article

## Crop plants transport irregularly shaped mineral particles from root to shoot: Tracking and quantifying

Jie Yang<sup>a,c</sup>, Lianzhen Li<sup>b</sup>, Chen Tu<sup>a,c</sup>, Ruijie Li<sup>a,c</sup>, Yongming Luo<sup>a,c,\*</sup><sup>a</sup> State Key Laboratory of Soil and Sustainable Agriculture, Institute of Soil Science, Chinese Academy of Sciences, Nanjing 210008, China<sup>b</sup> College of Environmental Sciences and Engineering, Qingdao University, Qingdao 266071, China<sup>c</sup> University of Chinese Academy of Sciences, Beijing 100049, China

## ARTICLE INFO

## Keywords:

Kaolin particles  
Wheat  
Lettuce  
Uptake and transport  
Translocation factors

## ABSTRACT

Mineral particles, ubiquitous in soils, influence crop plant growth by carrying nutrients and pollutants. While the uptake of dissolved mineral nutrients is well-established, the direct incorporation of irregular mineral particles into plants remains unclear. This study investigated the uptake and transport of kaolin particles, representative of minerals, by wheat and lettuce seedlings using hydroponic and soil cultures. Covalent labeling and advanced microscopy revealed that kaolin enters root steles at lateral root emergence sites, followed by transport to shoots. Fluorescent dyes and lanthanum (La)-labeled kaolin particles demonstrated that wheat surpassed lettuce in kaolin uptake in hydroponics, but both plants showed similar levels of particles in the shoots. Translocation factors (TFs) for kaolin were significantly higher in soil (0.089 for wheat, 0.039 for lettuce) compared to hydroponics (0.001 for wheat, 0.003 for lettuce). These findings provide compelling evidence for the direct uptake and transport of kaolin particles in crop plants. This opens new avenues for research on the interactions between plant and mineral particles, including other colloidal particles, in terrestrial ecosystems.

## 1. Introduction

Kaolin, a ubiquitous aluminosilicate mineral in soil, plays a multifaceted role in plant growth. Its positive impact derives from the ability of aluminosilicate minerals to retain mineral nutrients at the soil surface, preventing their migration to deep soil layers. These particles perform important functions in terrestrial biogeochemistry by interacting with organic matter and serving as a reservoir for mineral elements [1]. Conversely, kaolin acts as a carrier for immobile pollutants and biological pollutants, posing a threat to groundwater quality [2,3]. Current models of plant mineral nutrition focus on the acquisition of dissolved mineral ions or molecules. Studies have demonstrated that roots can take up aqueous  $\text{H}_4\text{SiO}_4$ , monomeric aluminum species, and soluble complexes via apoplastic pathway, with subsequent deposition as phytolith in the endodermis [4,5]. However, the potential contribution of sub-micron kaolin particles (a significant soil component) to plant uptake remains ambiguous and largely overlooked in terms of direct incorporation.

While the Casparian strips of the root endodermis are believed to act as a barrier to the apoplastic routes of exogenous particles into the root stele, the direct bioavailability of aluminosilicate mineral particles to

crop plants is still uncertain [6]. Discontinuous areas in the Casparian strips at the root apex and secondary root initiation sites might potentially facilitate the apoplastic route for the transportation of exogenous particles [7–9]. Recent research has shown that the cracks formed at new lateral root junctions can take up regular micrometer-sized plastics from soil and solution [10,11]. Several reports have suggested that some seaweeds or ferns can directly uptake particles from soil or saltwater based on the composition and pattern similarity of silicate particles to rare earth elements found in plants [12,13]. The fate of kaolin particles in crops after internalization remains unknown.

To elucidate plant kaolin uptake and transport, robust methods for particle tracking and quantification are required. Fluorescent labeling provides a simple and cost-effective approach. Additionally, rare earth elements (REEs) serve as promising quantitative tracers due to their low crustal abundance, low toxicity, and detectability at low concentrations (<1 ppb) [14]. One approach for labeling is to adsorb tracers onto minerals, which has been successfully applied in terrestrial and aquatic environments [14,15]. However, under complex rhizosphere conditions, these methods risk tracer dislodgment. The covalent attachment of markers to aluminosilicate minerals overcomes this limitation, providing a stable and reliable tracking method [16].

\* Corresponding author.

E-mail address: [ymluo@issas.ac.cn](mailto:ymluo@issas.ac.cn) (Y. Luo).<https://doi.org/10.1016/j.eehl.2024.05.002>

Received 10 January 2024; Received in revised form 13 April 2024; Accepted 4 May 2024

Available online 22 May 2024

2772-9850/© 2024 The Authors. Published by Elsevier B.V. on behalf of Nanjing Institute of Environmental Sciences, Ministry of Ecology and Environment (MEE) & Nanjing University. This is an open access article under the CC BY-NC-ND license (<http://creativecommons.org/licenses/by-nc-nd/4.0/>).

In this study, we employed covalent bonding of fluorescent dyes or REEs with kaolin particles to track and quantify their uptake and transport by crop plant [wheat (*Triticum aestivum*) and lettuce (*Lactuca sativa*)]. The objective of this study was to determine kaolin uptake in hydroponic and sandy soil systems using confocal laser scanning microscopy (CLSM) and advanced electron microscopy techniques. Additionally, we aimed to quantify plant kaolin content using REEs and inductively coupled plasma-mass spectrometry (ICP-MS), investigating direct assimilation and potential differences between plant types. Our findings will contribute to a deeper understanding of plant-mineral particle interactions, particularly the role of kaolin and other colloidal particles in terrestrial ecosystems.

## 2. Materials and methods

### 2.1. Kaolin particles and labeling

**Fluorescent-labeled kaolin particles:** Kaolin particles (Macklin Biochemical Co., Ltd, Shanghai, China) were labeled with Alexa Fluor 610-X NHS Ester (Thermo, USA) and aminopropyltriethoxysilane (APTS) through covalent bonding. The experimental procedures were as follows: 5.0 g of kaolin particles was dispersed in 20 mL of dry ethanol in a three-necked flask. Then, 10 mL of 3-aminopropyltriethoxysilane (APTS) was added under a nitrogen atmosphere, and the suspension was stirred and refluxed for 2 h at 80 °C. After the mixture cooled to room temperature ( $23 \pm 3$  °C), it was stirred overnight. The resultant mixture was centrifuged and extensively washed at least three times with deionized water to remove APTS. Then, the precipitates were dispersed in 10 mL of carbonate buffer solution (0.1 mol/L), and 30  $\mu$ L of Alexa Fluor 610-X NHS Ester (10 mg/mL) was added. The solution was shaken at 37 °C for 48 h. Finally, the labeled kaolin particles were purified using ethanol and deionized water under ultracentrifugation. The simplified synthesis route map of fluorescent-labeled kaolin particles is shown in Fig. S1a. The confocal laser scanning microscope (CLSM, FV1000, Olympus, Japan) was used to determine the fluorescence of minerals. To assess the stability of the fluorescent-labeled kaolin particles, the loss of fluorescent intensity of the fluorescent dye was measured after plant exposure to kaolin particles in the hydroponic solution for 24, 48, 96, 168, 240 h using a hybrid multi-mode microplate reader (SynergyH1, Biotek, USA). Each time, 4 mL of the exposure solution was taken and filtrated with a centrifugal ultrafiltration filter (3 kDa, Millipore, USA) at 4000 rpm for 10 min. The relative intensity was calculated as the fluorescent intensity of the dissolved dye (Alexa Fluor 610-X) as a percentage of the total fluorescent intensity in the fluorescent-labeled kaolin particles.

**La-labeled kaolin particles:** Lanthanum (La) was used for quantitative tracing of kaolin through covalent bonding with N-(trimethoxysilyl propyl) ethylenediamine triacetate (TMS-EDTA) as a bridge (Fig. S1b). The experimental procedures were as follows: 5.0 g of kaolin particles were dispersed in a mixture of 50 g methanol:water (85:15, v:v) under ultrasonication. The pH of the mixture was adjusted to 4.5 using HCl (0.5 mol/L). Then, 1 mL of TMS-EDTA was added, and the mixture was subjected to ultrasound for 10 min, 20  $\mu$ L glacial acetic acid was then added, and the mixture was stirred overnight at room temperature. The resultant mixture was centrifuged and washed at least three times with deionized water to remove TMS-EDTA. After dispersing in deionized water, the pH of the solution was adjusted to 6.0. Then, 10 mL lanthanum nitrate solution (200 mg/mL) was added, and the solution was stirred overnight. After the reaction, purification was performed by centrifugation. Finally, the surface adsorbed  $\text{La}^{3+}$  was removed after the initial La-labeled minerals were cleaned with 1 mM  $\text{NH}_4\text{NO}_3$ , accounting for 29.2% of the total concentration of La in the initial La-labeled kaolin particles, as determined by inductively coupled plasma-mass spectrometry (ICP-MS, ELAN DRC II, PerkinElmer, USA). The stability of La-labeled kaolin particles was detected in a plant-free hydroponic solution at different pH and exposure times. Kaolin particles exhibited good stability during the exposure period, particularly in pH 6.0–7.0

(<0.8 ppb) (Fig. S2). A digestion experiment was carried out to quantify the concentration of La in kaolin particles. 2 mL of different concentration labeled clay solutions (10, 50, 100, 200, and 500 mg/L) were digested by  $\text{HNO}_3$ , HCl, and  $\text{HClO}_4$  (digestion procedures are explained in the following section on plant digestion). The concentration of La was quantified using ICP-MS.

### 2.2. Kaolin characterization

Fourier-transform infrared spectroscopy (FTIR, Nicolet iS5, Thermo, USA) was used to analyze the surface groups of kaolin before the experiments ( $400\text{--}4000\text{ cm}^{-1}$ , 32 scans/sample) (Fig. S3a). X-ray diffraction (XRD, Smartlab 9, Rigaku, Japan) was used to determine kaolin phase structure [Cu-K $\alpha$  radiation,  $2\theta$  range  $5^\circ\text{--}90^\circ$ , PDF4+ database International Center for Diffraction Data (ICDD)] (Fig. S3b). Scanning electron microscopy (SEM, S-4800, Hitachi, Japan) with energy-dispersive X-ray spectroscopy (EDS, EX-350, Horiba, Japan) was used to analyze kaolin morphology and element distribution. The weight percentage [Wt(%)] of Al and Si in pristine kaolin were 15.55% and 16.84%; The Wt (%) of Al and Si in fluorescent-labeled kaolin were 11.33% and 11.17%; The Wt (%) of Al and Si in La labeled kaolin were 12.62% and 14.05%. Particle size was measured for 150 particles from multiple SEM images (Fig. S4). Zetasizer Nano ZS90 (Malvern Instrument, UK) was used to measure hydrodynamic diameter and zeta potential (Pristine kaolin:  $837.5 \pm 105.9\text{ nm}$ ,  $-35.5\text{ mV}$ ; Fluorescent-labeled kaolin:  $1292.3 \pm 155.6\text{ nm}$ ,  $37.3\text{ mV}$ ; La-labeled kaolin:  $796.3 \pm 40.1\text{ nm}$ ,  $-26.3\text{ mV}$ ). Specific surface area (SSA) was measured using  $\text{N}_2$  adsorption/desorption with Micromeritics (USA) ASAP 2460 (Table S1).

### 2.3. Crop plants and growth conditions

Seeds of wheat (*Triticum aestivum*) and lettuce (*Lactuca sativa*) were used in this study. All seeds were sterilized with NaClO solution [0.5% (w/v)] for 5 min. After rinsing, the wheat seeds were incubated on moist filter paper in the dark at room temperature for 4 d to accelerate germination. Then, six seedlings of uniform size were transferred into a 1 L beaker containing 600 mL of 1/5 hydroponic solution, consisting of an all-nutrient solution [5 mM  $\text{KNO}_3$ , 5 mM  $\text{Ca}(\text{NO}_3)_2 \cdot 4\text{H}_2\text{O}$ , 2 mM  $\text{MgSO}_4 \cdot 7\text{H}_2\text{O}$ , and 1 mM  $\text{KH}_2\text{PO}_4$ ] and micronutrients (0.045 mM  $\text{H}_3\text{BO}_3$ , 0.01 mM  $\text{MnCl}_2 \cdot 4\text{H}_2\text{O}$ , 0.8  $\mu\text{M}$   $\text{ZnSO}_4 \cdot 7\text{H}_2\text{O}$ , 0.3  $\mu\text{M}$   $\text{CuSO}_4 \cdot 5\text{H}_2\text{O}$ , 0.4  $\mu\text{M}$   $\text{Na}_2\text{MoO}_4 \cdot \text{H}_2\text{O}$ , and 0.02  $\mu\text{M}$  NaFe-EDTA) with the pH adjusted to 6.5. The pot was placed in a greenhouse with a light/dark cycle of 16/8 h, a temperature of  $25 \pm 2$  °C, and a relative humidity of 65%. After the seedlings grew lateral roots, the wheat was exposed to different particles (pristine kaolin particles, fluorescent-labeled kaolin particles, and La-labeled kaolin particles) in the hydroponic solution and soil matrix.

The lettuce seeds were cultured in organic soil (potting mix) in the greenhouse for 21 d. The seedlings were then removed from the soil and transferred to a 1 L beaker containing 1/5 strength hydroponic solution (600 mL). The roots were carefully rinsed and soaked with deionized water. Two lettuce plants of uniform size were allocated to grow for 3–5 d in the growth pot in the greenhouse before being exposed to different particles (same as wheat) in the hydroponic solution and soil matrix.

### 2.4. Kaolin particle exposures

#### 2.4.1. Pristine kaolin exposure

(1) In the hydroponic experiments, kaolin particles were added and ultrasonically dispersed in a 1/5 nutrient solution (250 mL beaker) at a concentration of 1.0 g/L. (2) In the soil experiments (200 g; pot container dimensions: 5 cm  $\times$  5 cm at the bottom; height: 8.7 cm), the content of kaolin particles was 1% (w/w) [The basic properties of sandy loam soil were as follows, pH: 8.9; TOC (total organic carbon): 3.3 g/kg; TN (total nitrogen): 0.25 g/kg; TP (total phosphorus): 0.23 g/kg. Mineral

composition of the soil: 42.1% quartz, 16.3% albite, 12.2% calcite, 6.3% microcline, 0.3% dolomite, 3.5% kaolinite, 18.7% muscovite, and 0.6%  $\text{Fe}_2\text{O}_3$ . Soil particle composition: 12.5% clay, 23.0% silt, and 64.5% sand]. The exposure periods for wheat and lettuce were 7 d or 14 d according to specific experiment.

#### 2.4.2. Fluorescent-labeled kaolin exposure

(1) In the hydroponic experiments, kaolin particles were added and ultrasonically dispersed in a 1/5 nutrient solution (250 mL beaker) at a concentration of 0.5 g/L (2) In the soil experiments, the condition was as described above, the content of fluorescent-labeled kaolin particles in the soil matrix (200 g) was 0.5% (w/w). (3) In the sand experiments, kaolin particles were added to the quartz sand matrix (200 g) at a concentration of 0.5% (w/w). Before adding the particles, quartz sand (380–830  $\mu\text{m}$ ) was soaked in 1%  $\text{HNO}_3$  overnight, washed with deionized water to achieve a pH of approximately 6.8, and then dried at 60 °C and cooled at room temperature. The Zeta potential of quartz sand was  $-17.6$  mV. The roots of wheat and lettuce were collected at different times (hydroponic experiment: 24 h, 48 h, 96 h, and 168 h; pot experiment: 7 d).

#### 2.4.3. La-labeled kaolin exposure

(1) In the hydroponic experiments, kaolin particles were added and ultrasonically dispersed in a 1/5 nutrient solution (250 mL beaker) at a concentration of 0.5 g/L. The 1/5 nutrient solution was renewed every 2 days. (2) In the soil experiments, the condition was as described above, and the content of La-labeled kaolin particles in the soil matrix (200 g) was 0.5% (w/w). Wheat and lettuce were collected after 7 d for the hydroponic experiments and 14 d for the pot experiments. In this section,

the pH of 1/5 nutrient solution was controlled using MES Buffer [2-(N-morpholino) ethane sulfonic acid (5 mM)].

#### 2.4.4. Quality assurance

In all experiments, blank controls (CK) were set up, where crop plants were untreated with kaolin particles, to monitor artifacts and possible background contamination. Each treatment was set in triplicate. In the hydroponic solution, all pots were manually stirred with a glass rod at regular intervals of 8 h to re-suspend and reduce the deposition of mineral particles at the bottom of the pot. After exposure, samples were obtained by carefully washing them with deionized water in a 250-mL glass beaker. In the case of the roots treated with La-labeled minerals, an additional procedure involving ultrasonic washing was implemented to ensure the plant surfaces were as clean as possible. In pot experiments, all samples were irrigated with 1/5 nutrient solution each day.

#### 2.5. Sample analysis procedures

##### 2.5.1. SEM observations of kaolin particles in plants

After the completion of the experiment, the samples were washed with deionized water. Roots, stems, and leaves samples were collected from wheat and lettuce seedlings treated with different treatments. Those samples were then cut into small pieces and cooled in liquid nitrogen, and freeze-dried for 24 h. Suspicious particles in crop plants were defined as those with a similar size and shape to pristine kaolin particles. They were identified in the vascular cylinder of plant lateral roots, stems, and leaves using SEM-EDS. After attaching the samples to the conductive adhesive, a 1-nm thick layer of Pt was sprayed. The Pt element was not shown in the results.

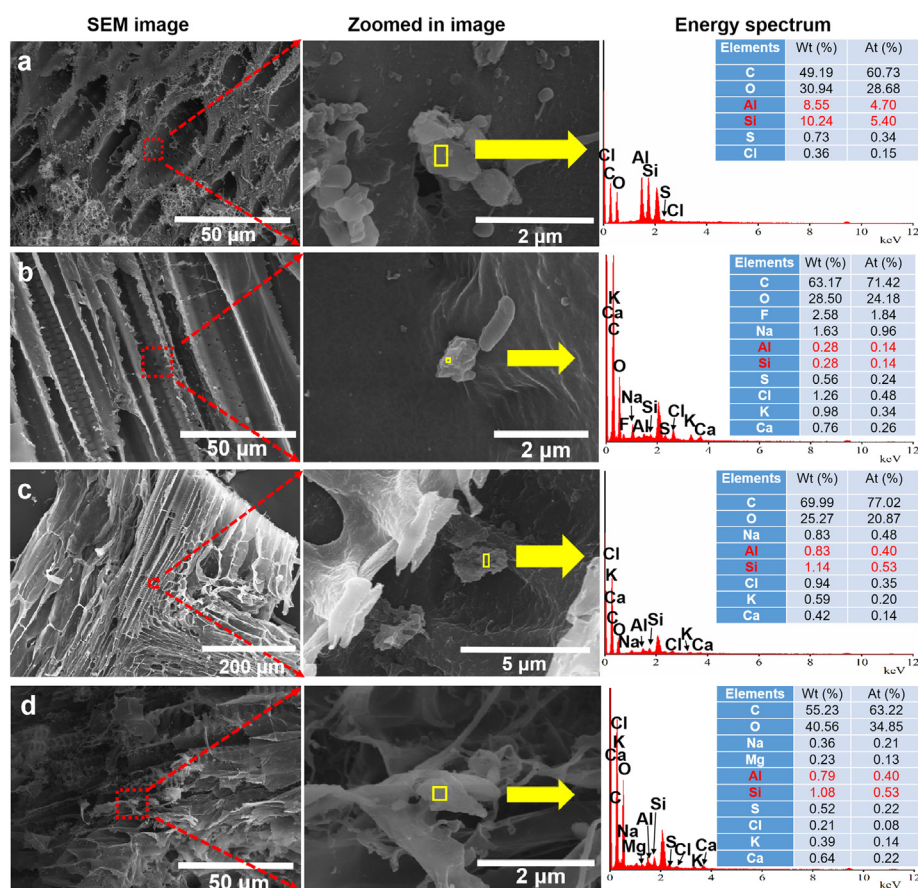


**Fig. 1.** SEM images of root steles showing kaolin particles in wheat and lettuce. Wheat was exposed to kaolin particles in hydroponic cultures (1.0 g/L, 7 d) (a), and sandy soils [1.0% (w/w), 14 d] (b). Lettuce was exposed to kaolin particles in hydroponic cultures (1.0 g/L, 7 d) (c) and sandy soils [1.0% (w/w), 14 d] (d). The left and middle columns are the SEM image and its zoomed-in image; the right column is the EDS spectra from the yellow rectangular area in the middle column.



### 2.5.2. TEM analysis of kaolin particles in xylem sap

After being exposed to 0 (untreated control) and 1.0 g/L pristine kaolin particles in a 1/5 nutrient solution for 14 d, xylem sap was carefully collected from wheat and lettuce. The collected xylem saps were then transferred and dispersed in ultrapure water. The bottom solution, after standing, was added to the copper grids for air-drying and analyzed using a field emission transmission electron microscope (FETEM, Thermo Scientific Talos F200X G2, USA). The sampling process of exudates was completed in an ultra-clean experimental room to prevent any contamination.

### 2.5.3. Localization of fluorescent kaolin particles in root

Roots from two separate batches of plant species were collected at different times (24 h, 48 h, 96 h, and 168 h) after exposure to fluorescent-labeled kaolin particles. The root apex, lateral root, and primary root of fresh roots were collected and embedded in 4% agarose. The samples were then transferred to a glass slide. To maintain the osmotic pressure balance in crop plants, a drop of 1X PBS buffer was added. The fluorescence of the transverse sections of the samples was then examined using CLSM (HeNe Red: 633 nm). The parameters were adjusted by deducting the auto-fluorescence of plant tissues from the samples in untreated controls.

### 2.5.4. Quantitative uptake and transport of kaolin particles

After being exposed to La-labeled kaolin particles for 14 d, the roots of crop seedling samples were either ultrasonically dispersed (for exposure to minerals) or soaked in a 10 mM EDTANa<sub>2</sub> solution (for exposure to La<sup>3+</sup> ions). The crop seedlings were then washed with distilled water. Subsequently, the seedlings were separated into roots, stems, and leaves and dried at 70 °C until a constant weight was achieved.

The digestion procedure for the samples was as follows: La-labeled kaolin particles and plant samples were predigested overnight in 3 mL of HNO<sub>3</sub> at room temperature. The samples were then heated at 180 °C on a hot plate for 2 h, followed by the addition of ~8 mL HCl:HNO<sub>3</sub> mixture (1:3; v:v), and 1 mL of HClO<sub>4</sub> was added successively for an additional 6 h to ensure complete digestion. After cooling, the digested solution was diluted and filtered (0.45 µm, Jinteng, China). The La contents were quantified using ICP-MS. Procedure blanks and certified reference materials (GBW100015a; Chinese Academy of Geological Sciences, China) were used for quality assurance and control (QA/QC). The recoveries of La ranged from 93.8% to 102.4%. The background La content of crop plants was determined by referring to the La content of crop plants in the untreated controls.

## 2.6. Statistical analyses

The data were preliminarily analyzed and integrated using Microsoft Excel (2016). The variability around the mean values was exhibited as  $\pm$  standard deviation. The content of both La and kaolin particles in plants was calculated by dry weight. Statistical analysis was performed using IBM SPSS Statistics 22. Duncan's test ( $p < 0.05$ , one-way ANOVA) was used to analyze the significant differences in the relative fluorescent intensity of fluorescent kaolin at different exposure times. The independent sample T-test analyzed the differences in the content of kaolin particles between wheat to lettuce. Origin 2021 software was used to visualize data.

## 3. Results

### 3.1. Tracking kaolin uptake in crop plants

Scanning electron microscopy (SEM) revealed suspicious particles resembling pristine kaolin in the steles of both wheat and lettuce roots exposed to kaolin in both hydroponics and soil (Fig. 1 and Figs. S5 and S6). Energy dispersive spectroscopy (EDS) confirmed that these particles

had Al-Si ratios matching those of pristine kaolin particles, verifying their presence within the plants.

Fluorescent-labeled kaolin particles exhibited strong fluorescence properties at an excitation wavelength of 633 nm (Fig. 2a) and The relative intensity of fluorescent-labeled kaolin treatment was not significantly different from the control treatment in the exposure solution during the 240 h exposure period. This demonstrates that fluorescent-labeled kaolin particles are very stable and have no leakage (Fig. 2b). Confocal laser scanning microscopy (CLSM) analysis with background bioluminescence subtraction revealed the distribution of labeled kaolin within roots (Fig. S7).

In hydroponics, the majority of the fluorescence signals occurred in the wheat and lettuce epidermis. Root apices had limited capacity to internalize and transport kaolin particles during the exposure period. Fluorescence was observed only in part of the root apices cortex and vascular tissue (such as wheat exposed to kaolin for 96 h) (Fig. S8). Clear fluorescence appeared in the lateral root junction after 96 h (Fig. 2c; Fig. S9). This exhibited a pathway for vascular tissue in crop plant roots through lateral root cracks that had not yet formed Casparian strips. In the primary root stele of crop plants, fluorescence mainly appeared in 168 h (Fig. S10). Pre-lateral root emergence exposure showed no stele uptake via apices (Fig. S11). Intriguingly, lettuce exhibited a relatively weaker fluorescence compared to wheat, suggesting differential uptake potential.

Furthermore, we exposed crop plants to fluorescent-labeled kaolin in soil. However, no detectable fluorescence was observed in the root of crop plant due to the interference from the soil inorganic and organic matter. Hence, we added sand experiments, and faint fluorescence confirmed that the lateral root junctions took up kaolin particles from quartz sands. Sand matrix exposure resulted in lower root kaolin content compared to hydroponics despite higher pot-concentration (Fig. S12).

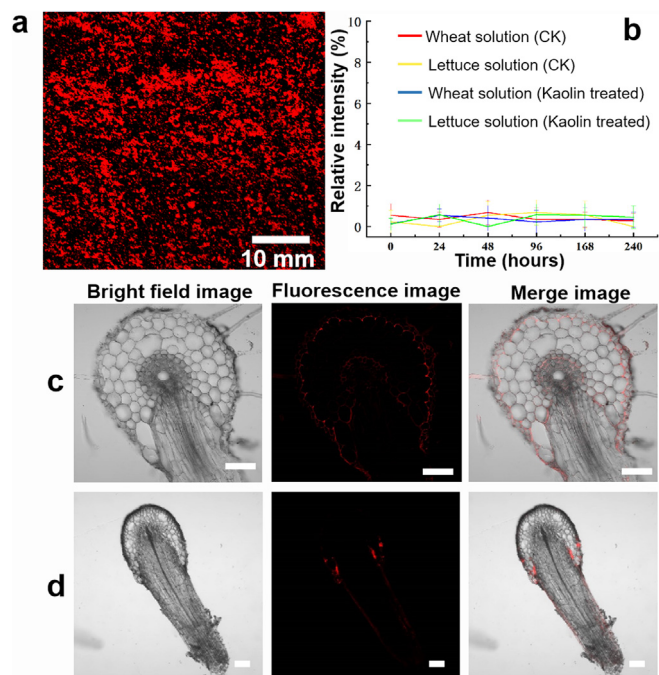


**Fig. 2.** Fluorescent labeling was used to track kaolin particles. A typical confocal microscope image of kaolin particles labeled with Alexa Fluor 610-X NHS ester was viewed using CLSM (a). Real-time monitoring of fluorescent dye leakage from labeled kaolin particles in wheat exposure solutions (b). Confocal images of transverse sections of wheat (c) and lettuce (d) roots that were treated by kaolin particles (0.5 g/L) at 96 h (The left column: bright-field images; the middle column: fluorescence images observed using CLSM; the right column: The corresponding merged images), Scale bars, 100 µm.

3.2. Tracking of kaolin transport in crop plants

Following internalization by roots, kaolin particles exhibited potential translocation to aerial parts. The SEM demonstrated the presence of diverse nutrient deposits in untreated controls (Figs. S13 and S14). Notably, after exposure to kaolin, both hydroponic and soil-grown plants displayed these particles within the vascular system of stems and leaves (Fig. 3, Fig. S15). Elemental analysis revealed the presence of K, Ca, Na, Mg, S, Cl, and others within these internalized particles. High-resolution transmission electron microscopy (HRTEM) further confirmed the presence of multiple nutrient deposits in the xylem sap of both wheat and lettuce (Fig. S16). Crystal structure analysis of the xylem sap in kaolin-treated plants provided solid evidence of the presence of kaolin particles (Fig. 4). Interestingly, these particles exhibited smoother surfaces and organic matter (C element) coating compared to their initial counterparts in the roots (Fig. S17). Moreover, essential nutrients like Ca, Fe, N, and S were observed deposited on their surfaces. These findings highlight the potential mobility of irregular kaolin particles within plant tissues.

3.3. Quantifying kaolin uptake and transport in crop plants

La was used as a tracer to chelate with silane covalently bound to kaolin particles for quantitative analysis of their uptake and transport in wheat and lettuce. La concentration in plant tissues served as an indicator of kaolin particle movement. La content in La-labeled kaolin particles was determined by digesting different contents of La-labeled kaolin particles (Fig. 5a). The stability of the La-labeled kaolin particles was tested in hydroponics and soil matrices throughout the incubation period (Tables S2 and S3). Supplementary experiments ruled out La ion interference in

uptake analysis (Fig. S18). Compared to plants exposed to dissolved La, those exposed to kaolin particles with La accumulated more La in their aboveground tissues, confirming the uptake of La-labeled kaolin.

Hydroponic exposure to La-labeled kaolin particles (0.50 g/L; 7 d) resulted in significant root accumulation in both wheat and lettuce (Fig. 5b; Table S4). After background La subtraction and La-to-kaolin conversion, most kaolin particles remained in the roots (wheat:  $21.6 \pm 10.1$  mg/g; lettuce:  $13.1 \pm 2.63$  mg/g). Shoot accumulation was minimal (wheat:  $0.03 \pm 0.00$  mg/g; lettuce:  $0.04 \pm 0.02$  mg/g). The translocation factors (TFs) for root-to-shoot transfer were minimal ( $<0.003$ ) in hydroponics, indicating limited translocation. In soil matrix exposure (0.5% w/w; 14 d), shoot accumulation increased for both wheat ( $0.45 \pm 0.04$  mg/g) and lettuce ( $0.42 \pm 0.13$  mg/g) (Fig. 5c). TFs reached 0.089 for wheat and 0.039 for lettuce, suggesting higher translocation compared to hydroponics.

4. Discussion

4.1. Redefining particle size limits in plant uptake

Traditionally, submicron particles were thought too large for direct internalization by plants due to the physical barriers like the cuticle, cell wall, and Casparian strip [17,18]. However, recent findings shed light on alternative pathways. Discontinuous areas in the Casparian strips of immature endodermal cells [9] and lateral root initiation sites [7,8] offer “crack-entry” routes for larger particles. Similar pathways facilitate pathogen and bacterial infections [19].

Microscopic and optical techniques have provided direct evidence that micro-sized plastics can accumulate at the junction of lateral roots and eventually enter a plant's vascular systems [10,20]. These openings

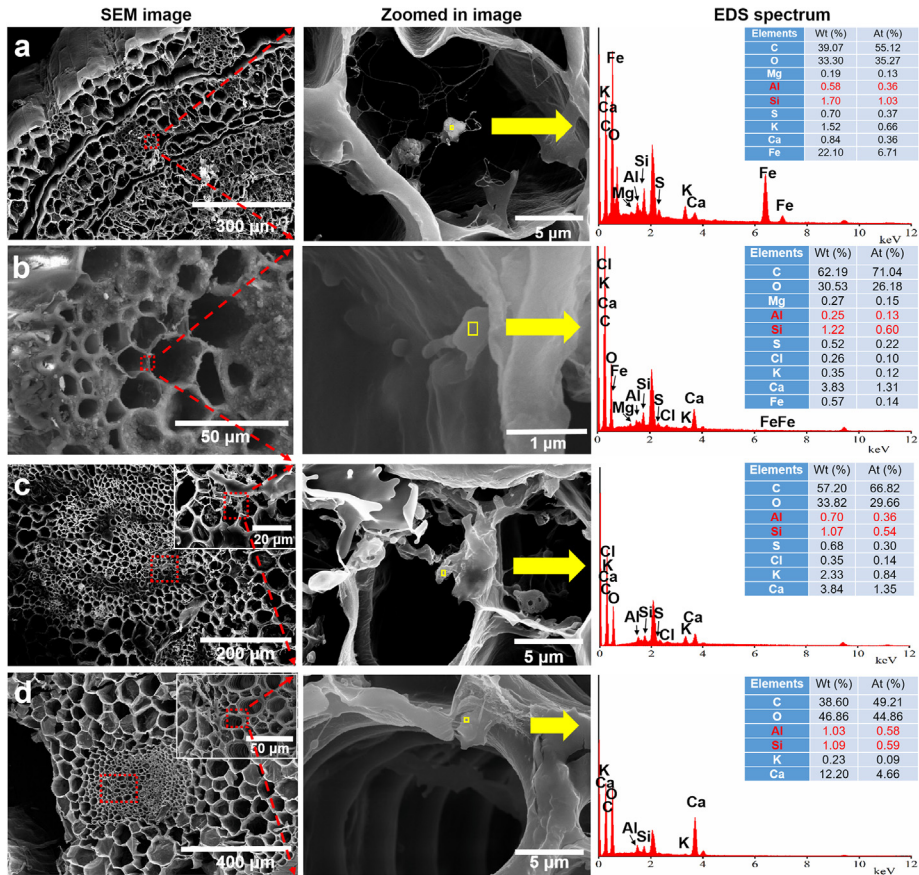
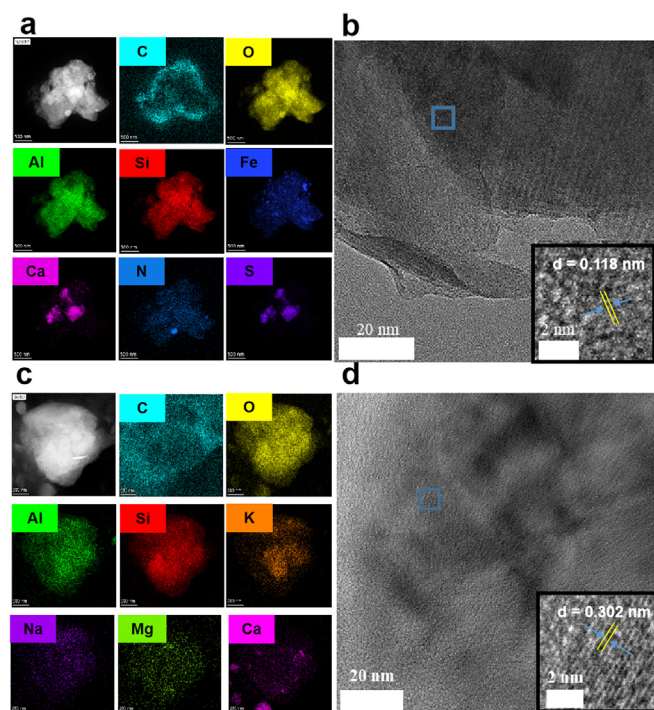


Fig. 3. SEM images and EDS analyses of kaolin particles in stem and leaf vasculatures. Wheat and lettuces were exposed to 1.0 g/L suspension of kaolin particles for 14 d. Wheat stem (a) and leaf (b) treated with kaolin particles; Lettuce stem (c) and leaf (d) treated with kaolin particles. The left and middle columns are SEM image and its zoomed-in image; the right column was the EDS spectra from the yellow rectangular area in the middle column.





**Fig. 4.** Scanning transmission electron microscopy (STEM) images of kaolin particles found in xylem sap in high-angle annular dark field (HAADF) mode and elemental mapping [including C, O, Al, Si, Fe, and others (K, Mg, Ca)] [wheat (a) and lettuce (c)]. Corresponding high-resolution transmission electron microscopy (HRTEM) images confirm the presence of particles with crystalline structures [wheat (b) and lettuce (d). Inset: the zoomed image of the region in the blue rectangle indicates this region has the crystal structure].

serve as pathways for infection by plant pathogens and bacteria, known as the “crack-entry” mode. In comparison to nonrigid polymer particles and microorganisms, kaolin particles have higher rigidity and irregular shapes. This unique crack entry pathway allows efficient uptake of kaolin particles that exceed the size exclusion limits for penetration of plant roots. Subsequently, these particles can be transported to aboveground tissues. Zhang and colleagues [21] found that a low content of CeO<sub>2</sub> NPs

could be transported aboveground. Lin and Xing [22] reported that only a few ZnO NPs were translocated from ryegrass roots to stems. Similarly, the content of Al maintains the same level when exposed to different contents of Al<sub>2</sub>O<sub>3</sub> NPs [23]. Based on the research conducted and previous research, the transport of particles from roots to aboveground tissues is limited. Micron-sized particles may be ingested less frequently than nano-sized particles [24], but their impact should not be ignored, especially considering the prevalence of micron-sized soil colloids in soils worldwide. Apart from abundant mineral colloids, many other colloids exist in the terrestrial system, such as oxide colloids, natural organic colloids, and bio-colloids [25]. The size boundaries for plant uptake of particulate matter need to be redefined.

#### 4.2. Crop plant interaction with kaolin particles

Crop plants play a vital role in human life, yet their interaction with ubiquitous kaolin particles, despite being chemically inert and non-toxic, has been largely overlooked. Different crop plants exhibit varying abilities to acquire kaolin particles. This study reveals fascinating differences in uptake capacity between wheat and lettuce, attributed to variations in root systems and exudates [wheat (a monocot) possesses a fibrous root system; lettuce (a dicot) has a taproot system] [26–28]. Preliminary result indicates that wheat, with its thin and dense root network, captures mineral particles more easily than lettuce in hydroponic solutions. However, lettuce roots exhibit a higher intake rate than wheat in soil matrices. Environmental factors also play a crucial role, as wheat and lettuce have higher TFs in soil matrices compare to hydroponic solutions. These differences may be related to exposure concentration, exposure period, and the strategies of plants to transport mineral particles to aboveground tissues, but this has to be explored yet.

This research also sheds light on a previously unrecognized pathway for plant nutrient acquisition. Si and Al, key components of kaolin particles, are typically absorbed as soluble silicic acid and dissolved Al [29, 30]. Our findings show direct uptake of solid-phase Si (submicro-sized mineral particles) at the site of lateral root emergence, supporting the work of Fu et al. [13] who observed silicate mineral particle incorporation. Another research also discovered that illite/muscovite is part of the mineral phases of phytoliths in partially mature wheat leaves [31]. These findings suggest kaolin minerals could be a significant Si source for plants [32]. Furthermore, the observed presence of elements like K, Ca, Na, Mg, S, Cl, Cu, and Fe on kaolin particles and their high specific surface area

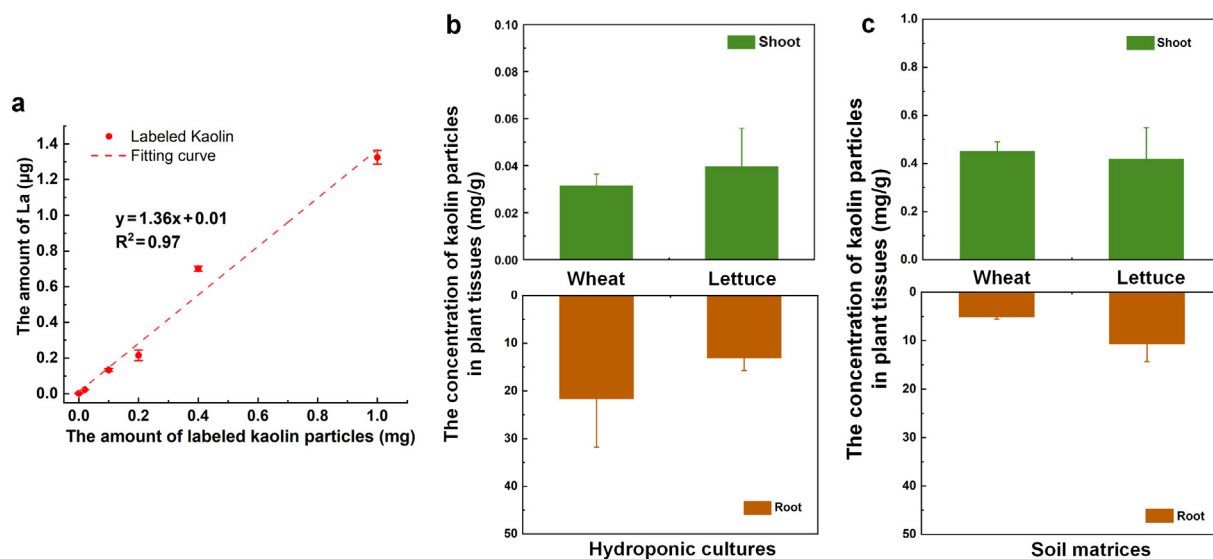


**Fig. 5.** Correlation between the calculated mass in suspensions of La-labeled kaolin particles (a). The content of kaolin particles (mg/g) in roots and aboveground tissues of plant in hydroponic (b) and soil systems (c). Wheat and lettuce were cultured in hydroponic solution and soil matrix [La-labeled kaolin particles content is 500 mg/L for 7 d and 0.5%(w/w) for 14 d]. The weight of plant was calculated by dry weight.

(SSA) point towards potential nutrient adsorption and delivery functionalities. This study reveals an important and previously unrecognized pathway for plant nutrient acquisition. Previous studies suggest plant interactions with mineral particles can influence plant metabolism and immunity [33], but understanding the transformation of minerals within complex plant tissues remains a challenge. It is unclear whether the deposition and release of mineral nutrients on clay minerals in wheat affect the uptake and transport of nutrients. Extensive research has shown that minerals play an important role in driving soil organic matter dynamics and stabilization [34–36]. However, the ingestion of particulate minerals by plant has been neglected, and the interactions between crop plants and mineral particles are not yet fully understood.

#### 4.3. Limitations and future perspective

While this study demonstrates submicron particle intake and transport by crop plants, the fate of these particles within the vascular system remains unclear. Additionally, potential interference between La-labeled minerals and bio-molecules requires further investigation. The long-term impacts of mineral particles on plant growth, nutrient cycling, and pollutant transport throughout the growth cycle also warrant exploration.

Despite these limitations, our findings highlight the significant role of the “crack-entry” mode in mineral particle uptake. Given the widespread presence of crop plants and the potential contribution of even small amounts of ingested minerals, further research is crucial to understand their involvement in nutrient acquisition, pollutant transport, and interactions with other colloidal particles like colloidal phosphorus and heavy metals.

Future research should focus on: (1) Understanding the fate of mineral particles within the plant's vascular system; (2) Investigating the positive and negative impacts of mineral particles on crop growth, nutrient cycling, and pollutant transport; (3) Exploring the interactions of crop plants with other colloidal particles in the soil, including colloidal phosphorus and heavy metals. This comprehensive exploration will shed light on the complex and previously unexamined interactions between crop plants and colloidal particles, contributing significantly to our understanding of plant and soil ecosystems.

#### 5. Conclusions

This study reveals the unexpected ability of wheat and lettuce seedlings to directly internalize and translocate kaolin particles. Our findings demonstrate that, beyond conventional size limitations, irregular kaolin particles can enter the root stele through “crack-entry” sites at lateral root emergence and subsequently be transported to the shoot. While wheat exhibited higher uptake in hydroponics, both plants accumulated comparable amounts in their aboveground tissues. Interestingly, the soil matrix significantly enhanced translocation compared to hydroponic cultures, highlighting the influence of exposure conditions on mineral particle uptake and transport. These findings shed new light on the complex interactions between mineral particles and plants in terrestrial ecosystems, opening promising avenues for further research on plant-environmental particle interactions within agroecosystems.

#### CRediT authorship contribution statement

**Jie Yang:** Data curation, Formal analysis, Investigation, Validation, Visualization, Writing – original draft. **Lianzhen Li:** Methodology, Writing – review & editing. **Chen Tu:** Writing – review & editing. **Ruijie Li:** Investigation. **Yongming Luo:** Conceptualization, Funding acquisition, Supervision, Writing – review & editing.

#### Declaration of competing interests

The authors have declared no conflicts of interest.

#### Acknowledgments

The financial support by the National Natural Science Foundation of China (41991330, 22241602, and 42177039) and the Postdoctoral Fellowship Program of CPSF (GZC20232783).

#### Appendix A. Supplementary data

Supplementary data to this article can be found online at <https://doi.org/10.1016/j.eehl.2024.05.002>.

#### References

- [1] B. Velde, P. Barré, *Soils, Plants and Clay Minerals*, Springer, Berlin, Heidelberg, 2010, p. 126, <https://doi.org/10.1007/978-3-642-03499-2>.
- [2] N.M. DeNovio, J.E. Saiers, J.N. Ryan, Colloid movement in unsaturated porous media: recent advances and future directions, *Vadose Zone J.* 3 (2) (2004) 338–351, <https://doi.org/10.2136/vzj2004.0338>.
- [3] J. Won, X. Wirth, S.E. Burns, An experimental study of cotransport of heavy metals with kaolinite colloids, *J. Hazard Mater.* 373 (2019) 476–482, <https://doi.org/10.1016/j.jhazmat.2019.03.110>.
- [4] M.J. Hodson, D.E. Evans, Aluminium/silicon interactions in higher plants, *J. Exp. Bot.* 46 (1995) 161–171, <https://doi.org/10.1093/jxb/era024>.
- [5] F. Guntzer, C. Keller, J.D. Meunier, Benefits of plant silicon for crops: a review, *Agron. Sustain. Dev.* 32 (2012) 201–213, <https://doi.org/10.1007/s13593-011-0039-8>.
- [6] J. Lv, S. Zhang, L. Luo, J. Zhang, K. Yang, P. Christie, Accumulation, speciation and uptake pathway of ZnO nanoparticles in maize, *Environ. Sci.: Nano* 2 (2015) 68–77, <https://doi.org/10.1039/C4EN00064A>.
- [7] J. Banda, K. Bellande, D. Wangenheim, T. Goh, S. Guyomarch, L. Laplace, M.J. Bennett, Lateral root formation in *Arabidopsis*: a well-ordered L-Rexit, *Trends Plant Sci.* 9 (24) (2019) 826–839, <https://doi.org/10.1016/j.tplants.2019.06.015>.
- [8] J. Lv, P. Christie, S. Zhang, Uptake, translocation, and transformation of metal-based nanoparticles in plants: recent advances and methodological challenges, *Environ. Sci.: Nano* 6 (2019) 41–59, <https://doi.org/10.1039/C8EN00645H>.
- [9] A. He, J. Jiang, J. Ding, G.D. Sheng, Blocking effect of fullerene nanoparticles (nC60) on the plant cell structure and its phytotoxicity, *Chemosphere* 278 (2021) 130474, <https://doi.org/10.1016/j.chemosphere.2021.130474>.
- [10] L. Li, Y. Luo, R. Li, Q. Zhou, W.J.G.M. Peijnenburg, N. Yin, J. Yang, C. Tu, Y. Zhang, Effective uptake of submicrometre plastics by crop plants via a crack-entry mode, *Nat. Sustain.* 3 (2020) 929–937, <https://doi.org/10.1038/s41893-020-0567-9>.
- [11] Y. Luo, L. Li, Y. Feng, R. Li, J. Yang, W. Peijnenburg, C. Tu, Quantitative tracing of uptake and transport of submicrometre plastics in crop plants using lanthanide chelates as a dual-functional tracer, *Nat. Nanotechnol.* 17 (2022) 424–431, <https://doi.org/10.1038/s41565-021-01063-3>.
- [12] F.F. Fu, T. Akagi, S. Yabuki, M. Iwaki, N. Ogura, Distribution of rare earth elements in seaweed: implication of two different sources of rare earth elements and silicon in seaweed, *J. Phycol.* 36 (2000) 62–70, <https://doi.org/10.1046/j.1529-8817.2000.99022.x>.
- [13] F.F. Fu, T. Akagi, S. Yabuki, Origin of silica particles found in the cortex of *matteuccia* roots, *Soil Sci. Soc. Am. J.* 66 (2002) 1265–1271, <https://doi.org/10.2136/sssaj2002.1265>.
- [14] K.L. Spencer, K. Suzuki, S. Hillier, The development of rare earth element-labelled potassium-depleted clays for use as cohesive sediment tracers in aquatic environments, *J. Soils Sediments* 11 (2011) 1052–1061, <https://doi.org/10.1007/s11368-011-0377-9>.
- [15] R.A. Hardy, J.M. Pates, J.N. Quinton, M.P. Coogan, A novel fluorescent tracer for real-time tracing of clay transport over soil surfaces, *Catena* 141 (2016) 39–45, <https://doi.org/10.1016/j.catena.2016.02.011>.
- [16] C.A. Diaz, Y.N. Xia, M. Rubino, R. Auras, K. Jayaraman, J. Hotchkiss, Fluorescent labeling and tracking of nanoclay, *Nanoscale* 5 (2013) 164, <https://doi.org/10.1039/C2NR32978F>.
- [17] F. Schwab, G. Zhai, M. Kern, A. Turner, J.L. Schnoor, M.R. Wiesner, Barriers, pathways and processes for uptake, translocation and accumulation of nanomaterials in plants – critical review, *Nanotoxicology* 10 (2016) 257–278, <https://doi.org/10.3109/17435390.2015.1048326>.
- [18] P. Zhang, Z. Guo, H. Fu, J.C. White, I. Lynch, Nanomaterial transformation in the soil–plant system: implications for food safety and application in agriculture, *Small* 16 (21) (2020) 2000705, <https://doi.org/10.1002/smll.202000705>.
- [19] S. Goormachtig, W. Capoen, M. Holsters, Rhizobium infection: lessons from the versatile nodulation behaviour of water-tolerant legumes, *Trends Plant Sci.* 9 (2004) 518–522, <https://doi.org/10.1016/j.tplants.2004.09.005>.
- [20] C. Zhang, N. Yue, X. Li, H. Shao, J. Wang, L. An, F. Jin, Potential translocation process and effects of polystyrene microplastics on strawberry seedlings, *J. Hazard Mater.* 449 (2023) 131019, <https://doi.org/10.1016/j.jhazmat.2023.131019>.
- [21] Y. Zhang, F. Hou, Y. Tan, CeO<sub>2</sub> nanoplates with a hexagonal structure and their catalytic applications in highly selective hydrogenation of substituted nitroaromatics, *Chem. Commun.* 48 (2012) 2391–2393, <https://doi.org/10.1039/C1CC16983A>.
- [22] D. Lin, B. Xing, Root uptake and phytotoxicity of ZnO nanoparticles, *Environ. Sci. Technol.* 42 (15) (2008) 5580–5585, <https://doi.org/10.1021/es800422x>.
- [23] K.L. Hayes, J. Mui, B. Song, E.S. Sani, S.W. Elsenman, J.B. Kim, Effects, uptake, and translocation of aluminum oxide nanoparticles in lettuce: a comparison

- study to phytotoxic aluminum ions, *Sci. Total Environ.* 719 (2020) 137393, <https://doi.org/10.1016/j.scitotenv.2020.137393>.
- [24] H. Li, X. Chang, J. Zhang, Y. Wang, R. Zhong, L. Wang, J. Wei, Y. Wang, Uptake and distribution of microplastics of different particle sizes in maize (*Zea mays*) seedling roots, *Chemosphere* 313 (2023) 137491, <https://doi.org/10.1016/j.chemosphere.2022.137491>.
- [25] J.F. McCarthy, et al., Colloid transport in the subsurface: past, present, and future challenges, *Vadose Zone J.* 3 (2004) 326–337, <https://doi.org/10.2136/vzj2004.0326>.
- [26] R. Crang, S. Lyons-Sobask, R. Wise, *Plant Anatomy: A Concept-Based Approach to the Structure of Seed Plants*, Springer, 2018, <https://doi.org/10.1007/978-3-319-77315-5>.
- [27] E. Spielman-Sun, A. Avellan, G.D. Bland, R.V. Tappero, A.S. Acerbo, J.M. Unrine, J.P. Giraldo, G.V. Lowry, Nanoparticle surface charge influences translocation and leaf distribution in vascular plants with contrasting anatomy, *Environ. Sci.: Nano* 6 (8) (2019) 2508–2519, <https://doi.org/10.1039/C9EN00626E>.
- [28] P. Zhang, Y. Ma, C. Xie, Z. Guo, X. He, E. Valsami-Jones, I. Lynch, W. Luo, L. Zheng, Z. Zhang, Plant species-dependent transformation and translocation of ceria nanoparticles, *Environ. Sci.: Nano* 6 (2019) 60–67, <https://doi.org/10.1039/C8EN01089G>.
- [29] J. Ma, N. Yamaji, Silicon uptake and accumulation in higher plants, *Trends Plant Sci.* 11 (8) (2006) 392–397, <https://doi.org/10.1016/j.tplants.2006.06.007>.
- [30] R. Rahman, H. Upadhyaya, Aluminium toxicity and its tolerance in plant: a review, *J. Plant Biol.* 64 (2021) 101–121, <https://doi.org/10.1007/s12374-020-09280-4>.
- [31] N.C. Andriopoulou, G.E. Christidis, Multi-analytical characterisation of wheat biominerals: impact of methods of extraction on the mineralogy and chemistry of phytoliths, *Archaeol. Anthropol. Sci.* 12 (2020) 186, <https://doi.org/10.1007/s12520-020-01091-5>.
- [32] C. Keller, M. Rizwan, J.D. Meunier, Are clay minerals a significant source of Si for crops? A comparison of amorphous silica and the roles of the mineral type and pH, *Silicon* 13 (2021) 3611–3618, <https://doi.org/10.1007/s12633-020-00877-5>.
- [33] S. Anne-Désirée, G. Sophele, B. Jean-Michel, N. Nicolas, T. Emmanuel, Calcium isotope fractionation associated with adsorption and desorption on/from  $\delta$ -MnO<sub>2</sub>, *Geochem. Cosmochim. Acta* 354 (2023) 109–122, <https://doi.org/10.1016/j.gca.2023.06.003>.
- [34] J.Q. Yang, X. Zhang, L.C. Bourg, H.A. Stone, 4D imaging reveals mechanisms of clay-carbon protection and release, *Nat. Commun.* 12 (2021) 622, <https://doi.org/10.1038/s41467-020-20798-6>.
- [35] M. Yu, Y. Hua, M.T. Sarwar, H. Yang, Nanoscale interactions of humic acid and minerals reveal mechanisms of carbon protection in soil, *Environ. Sci. Technol.* 57 (1) (2023) 286–296, <https://doi.org/10.1021/acs.est.2c06814>.
- [36] S. Wu, K.O. Konhauser, B. Chen, L. Huang, “Reactive Mineral Sink” drives soil organic matter dynamics and stabilization, *npj Mater. Sustain.* 1 (2023) 3, <https://doi.org/10.1038/s44296-023-00003-7>.